

快速收敛的四边形网格三分细分模式*

刘 丽^{1,2}, 张彩明¹⁺, 杨兴强¹, 伯彭波³

¹(山东大学 计算机科学与技术学院, 山东 济南 250061)

²(山东师范大学 信息科学与工程学院, 山东 济南 250014)

³(香港大学 计算机科学系, 香港)

Ternary Subdivision Scheme for Quadrilateral Mesh with Fast Convergence

LIU Li^{1,2}, ZHANG Cai-Ming¹⁺, YANG Xing-Qiang¹, BO Peng-Bo³

¹(School of Computer Science and Technology, Shandong University, Ji'nan 250061, China)

²(School of Information Science and Engineering, Shandong Normal University, Ji'nan 250014, China)

³(Department of Computer Science, University of Hong Kong, Hong Kong, China)

+ Corresponding author: Phn: +86-531-88395773, Fax: +86-531-82602656, E-mail: czhang@sdu.edu.cn

Liu L, Zhang CM, Yang XQ, Bo PB. Ternary subdivision scheme for quadrilateral mesh with fast convergence. *Journal of Software*, 2007,18(9):2346-2355. <http://www.jos.org.cn/1000-9825/18/2346.htm>

Abstract: This paper proposes a ternary stationary subdivision scheme for quadrilateral mesh. For regular and irregular quadrilateral meshes, different subdivision masks are applied to generate new vertices. The number of faces on the refined mesh is about nine times than that of the coarse mesh after every subdivision step. The limit surface generated by the new method is C^2 continuous for a regular mesh and C^1 continuous for an irregular mesh. Compared with typical subdivision schemes, the proposed scheme has faster convergence speed and the ability to solve arbitrary topological quadrilateral mesh. Some examples are given in the end to illustrate the performance of the new subdivision scheme.

Key words: discrete Fourier transform; ternary subdivision; quadrilateral mesh; eigenvalue

摘要: 提出了四边形网格的三分细分模式,对于正则和非正则四边形网格,分别采用不同的细分模板获得新的细分顶点,从双三次B样条中推导出正则四边形网格的三分细分模板,极限曲面 C^2 连续;对细分矩阵进行傅里叶变换,推导出非正则四边形网格的三分细分模板,极限曲面 C^1 连续.提出的三分细分模式可以解决任意拓扑四边形网格的曲面细分问题.与其他细分模式相比,具有收敛速度快、适用范围广等优点.最后给出了四边形网格细分的实例.

关键词: 离散傅里叶变换;三分细分;四边形网格;特征值

中图法分类号: TP391 文献标识码: A

* Supported by the National Basic Research Program of China under Grant No.2006CB303102 (国家重点基础研究发展计划(973)); the National Natural Science Foundation of China under Grant Nos.60673003, 60573180 (国家自然科学基金)

Received 2006-05-11; Accepted 2006-11-03

1 Introduction

Subdivision schemes have been widely used for shape modeling due to their advantages in dealing with meshes of arbitrary topologies. Subdivision surfaces have the benefits of both polygons and spline surfaces, and it allows the users to generate smooth surfaces through a small set of control vertices. Its ability of integrating continuous surface models with discrete representations leads to simple and efficient algorithms.

Since the introduction of Catmull-Clark subdivision surfaces at the end of the 1970s^[1], many subdivision schemes have been proposed for various applications. For a quadrilateral mesh, Catmull-Clark subdivision produces uniform bi-cubic B-spline surfaces and Doo-Sabin subdivision^[2] generates uniform bi-quadratic B-spline surfaces. There are a rich family of subdivision schemes available now^[3], such as classical schemes and combined schemes^[4-15]. These methods are widely used in geometric design and computer graphics area for shape design, animation, multi-resolution modeling and many other engineering applications. Some extensions to meshes with arbitrary topologies and shape features make subdivision surfaces a more valuable asset in application.

For subdivision schemes, the control meshes are continuously refined in each step so that finer meshes are generated. The face number and vertex number increase rapidly with the subdivision process. Many researchers investigate schemes with an odd number of control points and work out a more general ternary subdivision scheme. Hassan^[16] proposes a ternary subdivision scheme that can only work on regular meshes. Maillot and Stam^[17] give a general subdivision scheme that allows any degree of refinements in a single step. However, the properties of the limit surfaces are not studied. In this paper, we use different masks to subdivide regular and irregular meshes and prove that the limit surfaces generated by the new scheme are C^2 and C^1 respectively.

The rest of the paper is organized as follows. In Section 2, we present a new ternary subdivision scheme for regular and irregular meshes. Its convergence is proved and the continuity condition of the limit surface is also given. In Section 3, the proposed subdivision scheme is compared with other subdivision schemes, and some examples are presented. Finally, we draw conclusions in Section 4.

2 A Ternary Stationary Subdivision Scheme

A subdivision rule is an algorithm that produces a finer mesh with more details from an original coarse mesh, where the connectivity information and the geometric information are applied. Given a simplicial complex $K=(V,E,F)$ and a quadrilateral mesh $M=(K,\Phi)$, a vertex is called a regular vertex if it is an interior vertex and has the degree of 4 or it is a boundary vertex and has the degree of 3 or 2; otherwise, the vertex is called an extraordinary vertex. A mesh without extraordinary vertices is called a regular mesh; otherwise, it is called an irregular mesh. In this section, we propose subdivision masks for regular and irregular meshes.

2.1 Subdivision scheme for regular mesh

Regular mesh can be expressed as the form of tensor product surface by taking mesh vertices as control points. Bi-cubic B-spline surface based on quadrilateral mesh with 16 control points can be formulated as

$$S(u,v)=UMGM^T V \tag{1}$$

where $M = \frac{1}{6} \begin{bmatrix} -1 & 3 & -3 & 1 \\ 3 & -6 & 3 & 0 \\ -3 & 0 & 3 & 0 \\ 1 & 4 & 1 & 0 \end{bmatrix}$ is the matrix of the basis function, $G = \begin{bmatrix} P_{11} & P_{12} & P_{13} & P_{14} \\ P_{21} & P_{22} & P_{23} & P_{24} \\ P_{31} & P_{32} & P_{33} & P_{34} \\ P_{41} & P_{42} & P_{43} & P_{44} \end{bmatrix}$ is the matrix of

control points, $U=[u^3 \ u^2 \ u \ 1], V=[v^3 \ v^2 \ v \ 1]^T$ are parameter vectors.

Setting $u_1=u/3, v_1=v/3$, the bi-cubic B-spline surface can be expressed as

$$S(u_1, v_1) = USMG M^T S V \tag{2}$$

where $S = \begin{bmatrix} 1/27 & 0 & 0 & 0 \\ 0 & 1/9 & 0 & 0 \\ 0 & 0 & 1/3 & 0 \\ 0 & 0 & 0 & 1 \end{bmatrix}$.

Refining the original control mesh leads to the new F-vertices, E-vertices and V-vertices, but the spline surfaces are the same, so we can obtain

$$S(u_1, v_1) = UMG_1 M^T V = USMG M^T S V \tag{3}$$

Thus the subdivision control points G_1 can be expressed as

$$G_1 = [M^{-1} S M] G [M^T S (M^T)^{-1}] = H_1 G H_1^T \tag{4}$$

where $H_1 = M^{-1} S M = \frac{1}{27} \begin{bmatrix} 10 & 16 & 1 & 0 \\ 4 & 19 & 4 & 0 \\ 1 & 16 & 10 & 0 \\ 0 & 10 & 16 & 1 \end{bmatrix}$.

The new control point q_{ij} is generated by the control point P_{ij} and its neighbor points multiplied by corresponding coefficient A_{ij} . According to Eq.(4), we can get the coefficient A_{ij} and their relationship as follows

$$\begin{aligned} A_{11} = A_{13} = A_{14} = A_{31} = A_{33} = A_{34} = A_{41} = A_{43} = A_{44} &= \frac{1}{729} [100 \ 160 \ 10 \ 160 \ 256 \ 16 \ 10 \ 16 \ 1] \\ A_{12} = A_{21} = A_{23} = A_{24} = A_{32} = A_{42} &= \frac{1}{729} [40 \ 190 \ 40 \ 64 \ 304 \ 64 \ 4 \ 19 \ 4] \\ A_{22} &= \frac{1}{729} [16 \ 76 \ 16 \ 76 \ 361 \ 76 \ 16 \ 76 \ 16] \end{aligned} \tag{5}$$

The new face vertices $q_{11}, q_{13}, q_{14}, q_{31}, q_{33}, q_{34}, q_{41}, q_{43}, q_{44}$ and the new edge vertices $q_{12}, q_{21}, q_{23}, q_{24}, q_{32}, q_{42}$ (Fig.1) have the same coefficients respectively, so we get the subdivision masks for regular mesh as shown in Fig.2.

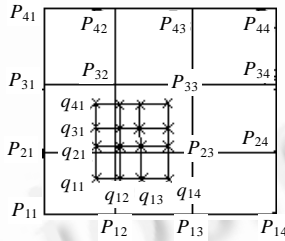


Fig.1 Bi-Cubic spline subdivision scheme of regular mesh

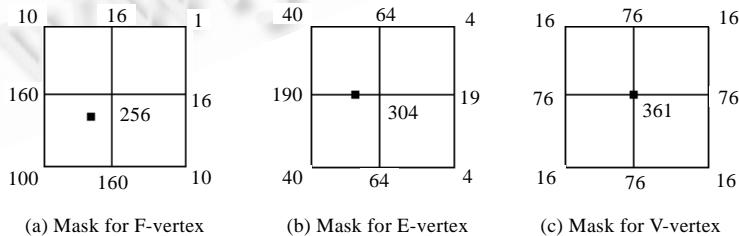


Fig.2 Masks of regular mesh

The refined control point G_1 is deduced from the expression of spline surface, so the limit surface generated by this scheme is also bi-cubic B-spline surface. To subdivide the same original mesh, the ternary scheme generates the same limit surface as Catmull-Clark subdivision, so the limit surface is also C^2 continuous.

2.2 Subdivision scheme for irregular mesh

To define a subdivision scheme for irregular mesh, we need to specify rules for computing positions of the new vertices and rules to update the positions of the existing vertices. When new vertices inserted on each edge and face are connected by edges, each face is partitioned into 9 quads using the ternary subdivision scheme. The subdivision rules that we propose are the following

Face rule: The F-vertex v_f near the vertex v_0 is computed by the following formula (Fig.3(a)).

$$v_f = \frac{1}{9}(4v_0 + 2v_1 + v_2 + 2v_3) \tag{6}$$

Edge rule: The E-vertex v_e near the vertex v_0 can be computed by the linear combination of the vertices corresponding to the edge (Fig.3(b))

$$v_e = \frac{1}{15}(6v_0 + 3v_1 + v_2 + 2v_3 + v_4 + 2v_5) \tag{7}$$

Vertex rule: the new position of the V-vertex v_v can be determined by the linear combination of the old vertex v and its 1-neighborhood, which include immediate and diagonal vertices (Fig.3(c)).

$$v_v = (1 - \alpha - \beta)v + \frac{1}{n} \sum_{i=0}^{n-1} \alpha v_{2i} + \frac{1}{n} \sum_{i=0}^{n-1} \beta v_{2i+1} \tag{8}$$

where n is the valence of the vertex v , α and β are two free parameters which are obtained by considering the convergence of the subdivision scheme and the continuous condition of the limit surface. Note that during the process of iterative refinements, the valence of each original vertex is invariable.

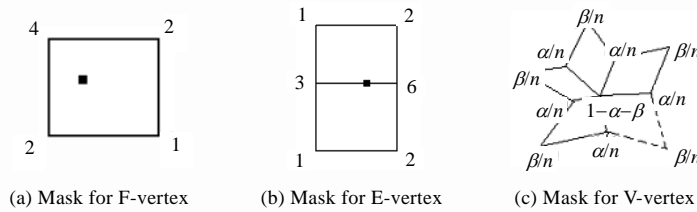


Fig.3 Masks of irregular mesh

2.3 Convergence proof and continuity analysis

The eigenstructure of subdivision matrices is necessary for the convergence proof and continuity analysis of the limit surface, so we firstly deduce the eigenstructure of the subdivision matrices of the ternary scheme. To simplify computation of the eigenvalues, the vertex $V^{(k)}$ at the k -th subdivision level is used n times, and then the iteration rule of vertex computation is

$$V^{(k)} = \sum_{j=0}^{n-1} S_j^{(k)} V^{(k-1)} \tag{9}$$

where $S_i^{(k)}$ ($i=0, \dots, n-1$) are block matrices of the k -th level subdivision matrix $S^{(k)}$, and can be expressed as

$$S_0^{(k)} = \begin{bmatrix} (1-\alpha-\beta)/n & \alpha/2n & \beta/n & \alpha/2n \\ 1/5 & 1/10 & 1/15 & 2/15 \\ 4/9 & 2/9 & 1/9 & 2/9 \\ 1/5 & 2/15 & 1/15 & 1/10 \end{bmatrix}, \quad S_1^{(k)} = \begin{bmatrix} (1-\alpha-\beta)/n & \alpha/2n & \beta/n & \alpha/2n \\ 0 & 0 & 0 & 0 \\ 0 & 0 & 0 & 0 \\ 1/5 & 1/10 & 1/15 & 2/15 \end{bmatrix}, \tag{10}$$

$$S_i^{(k)} = \begin{bmatrix} (1-\alpha-\beta)/n & \alpha/2n & \beta/n & \alpha/2n \\ 0 & 0 & 0 & 0 \\ 0 & 0 & 0 & 0 \\ 0 & 0 & 0 & 0 \end{bmatrix} \quad (i=2, \dots, n-2), \quad S_{n-1}^{(k)} = \begin{bmatrix} (1-\alpha-\beta)/n & \alpha/2n & \beta/n & \alpha/2n \\ 1/5 & 2/15 & 1/15 & 1/10 \\ 0 & 0 & 0 & 0 \\ 0 & 0 & 0 & 0 \end{bmatrix}$$

The subdivision matrix $S^{(k)} = bcirc(S_0^{(k)}, S_1^{(k)}, \dots, S_{n-1}^{(k)})$ is transformed into block diagonal matrix $\tilde{S}^{(k)} = bcirc(\tilde{S}_0^{(k)}, \tilde{S}_1^{(k)}, \dots, \tilde{S}_{n-1}^{(k)})$ by Discrete Fourier Transform (DFT). The relationship between the subdivision matrix and diagonal matrix is the following

$$S^{(k)} = U\tilde{S}^{(k)}U^T \tag{11}$$

where $U = \frac{1}{\sqrt{n}} \begin{bmatrix} 1 & 1 & \dots & 1 \\ 1 & \omega & \dots & \omega^{n-1} \\ \vdots & \vdots & \ddots & \vdots \\ 1 & \omega^{n-1} & \dots & \omega^{(n-1)^2} \end{bmatrix}$, $\tilde{S}^{(k)} = \frac{1}{n} \sum_{j=0}^{n-1} S_j^{(k)} \omega^{ij}$, $j = 0, 1, \dots, n-1$.

DFT is used here as an algebraic tool to transform subdivision scheme into a form suitable for the analysis. This allows us to formulate simple and numerically sufficient criteria for the convergence of subdivision scheme. The matrices $S^{(k)}$ and $\tilde{S}^{(k)}$ are similar ones and have the same eigenvalues, so we can analyze the eigenvalue spectrum of the matrix $\tilde{S}^{(k)}$ instead of $S^{(k)}$. The block matrices of the diagonal matrix $\tilde{S}^{(k)}$ are

$$\tilde{S}_0^{(k)} = S_0^{(k)} + S_1^{(k)} + (n-3)S_1^{(k)} + S_{n-1}^{(k)} \tag{12}$$

$$\tilde{S}_i^{(k)} = S_0^{(k)} + \omega^{-i}S_1^{(k)} - (1 + \omega^i + \omega^{-i})S_1^{(k)} + \omega^i S_{n-1}^{(k)}, (i = 1, \dots, n-1) \tag{13}$$

Using Eq.(10) and Eq.(12), we get

$$\tilde{S}_0^{(k)} = S_0^{(k)} + S_1^{(k)} + (n-3)S_1^{(k)} + S_{n-1}^{(k)} = \begin{pmatrix} 1-\alpha-\beta & \alpha/2 & \beta & \alpha/2 \\ 2/5 & 7/30 & 2/15 & 7/30 \\ 4/9 & 2/9 & 1/9 & 2/9 \\ 2/5 & 7/30 & 2/15 & 7/30 \end{pmatrix}$$

The eigenvalues of matrix $\tilde{S}_0^{(k)}$ are $\lambda_0=1$,

$$\lambda_1 = \frac{\alpha}{2} + \frac{13}{45} - \frac{\beta}{2} + \frac{1}{90} \sqrt{2025\alpha^2 - 2520\alpha + 4050\alpha\beta + 736 - 2160\beta + 2025\beta^2},$$

$$\lambda_2 = -\frac{\alpha}{2} + \frac{13}{45} - \frac{\beta}{2} - \frac{1}{90} \sqrt{2025\alpha^2 - 2520\alpha + 4050\alpha\beta + 736 - 2160\beta + 2025\beta^2},$$

$$\lambda_3 = 0.$$

Setting $\alpha=4/9$ and $\beta=4/45$, we have $2025\alpha^2 - 2520\alpha + 4050\alpha\beta + 736 - 2160\beta + 2025\beta^2 = 0$, then the eigenvalues of $\tilde{S}_0^{(k)}$ are 0, 1, 1/45, 1/45, respectively. By (10) and (13), we have

$$\begin{aligned} \tilde{S}_i^{(k)} &= S_0^{(k)} + \omega^{-i}S_1^{(k)} + (1 + \omega^i + \omega^{-i})S_1^{(k)} + \omega^i S_{n-1}^{(k)} \\ &= \begin{pmatrix} 1-\alpha-\beta & \alpha/2 & \beta & \alpha/2 \\ 1/5 + \omega^i/5 & 1/10 + 2\omega^i/15 & 1/15 + \omega^i/15 & 2/15 + \omega^i/10 \\ 4/9 & 2/9 & 1/9 & 2/9 \\ \omega^{-i}/5 + 1/5 & \omega^{-i}/10 + 2/15 & \omega^{-i}/15 + 1/15 & 2\omega^{-i}/15 + 1/10 \end{pmatrix} \end{aligned}$$

The eigenvalues of the matrix $\tilde{S}_i^{(k)}$ are $\lambda_{i0}=1/90$

$$\lambda_{i1} = \frac{1}{270\omega^i(102\omega^i + 18 + 18\omega^{2i} - \sqrt{6(322\omega^{2i} + 72\omega^i + 72\omega^{3i} + 9 + 9\omega^{4i}))}},$$

$$\lambda_{i2} = \frac{1}{270\omega^i(102\omega^i + 18 + 18\omega^{2i} + \sqrt{6(322\omega^{2i} + 72\omega^i + 72\omega^{3i} + 9 + 9\omega^{4i}))}},$$

$$\lambda_{i3} = 0.$$

Since the matrices $S^{(k)}$ and $\tilde{S}^{(k)}$ are similar ones, the eigenvalues of the matrix $S^{(k)}$ are the same as those of the matrix $\tilde{S}^{(k)}$. Similar to the uniform stationary subdivision scheme, the subdivision matrices of different levels satisfy $S=S^{(1)}=\dots=S^{(k)}$, so the eigenvalues of subdivision matrix S satisfy

$$\lambda_0=1 > \lambda_1 = \lambda_2 > \|\lambda_{i0}\| \geq \|\lambda_{i1}\| \geq \|\lambda_{i2}\| \geq \|\lambda_{i3}\| = 0, i = 1, \dots, n-1.$$

After getting the eigenstructure, the convergence analysis of the ternary subdivision scheme can be performed by analyzing the eigenvalues of the subdivision matrix S .

Theorem 1. The limit surface of the ternary subdivision scheme is convergent.

Proof: The vector of initial data can be decomposed into eigenvector \mathbf{d}_i scaled by weight $\mathbf{a}_i \in \mathbb{R}^3$ called eigencoefficient, the vertex $V^{(0)}$ satisfies

$$V^{(0)} = \sum_{i=0}^{n-1} \mathbf{a}_i \mathbf{d}_i \tag{14}$$

Note that \mathbf{a}_i is a row vector, hence

$$V^{(k)} = S V^{(k-1)} = \dots = S^{(k)} V^{(0)} = \sum_{i=0}^{n-1} \mathbf{a}_i \lambda_i^k \mathbf{d}_i = \lambda_0^k \left(\mathbf{a}_0 \mathbf{d}_0 + \sum_{i=0}^{n-1} \left(\frac{\lambda_i}{\lambda_0} \right) \mathbf{a}_i \mathbf{d}_i \right) \tag{15}$$

The eigenvalues of the subdivision matrices satisfy $\lambda_0^{(k)} = 1$ and $\lim_{k \rightarrow \infty} \lambda_i^{(k)} = 0 (i \neq 0)$, so we get

$$\lim_{k \rightarrow \infty} V^{(k)} = \mathbf{a}_0 \mathbf{d}_0 \tag{16}$$

Therefore, we draw a conclusion that the new ternary stationary subdivision scheme is convergent. □

Theorem 2. The subdivision scheme defined by irregular subdivision masks is C^1 continuous.

Proof: Let $V_l^{(k)}, V_t^{(k)}$ be the l -th and t -th components of the vertex $V^{(k)}$, d_{il}, d_{it} be the l -th and t -th components of the eigenvector \mathbf{d}_i , respectively. With $\mathbf{d}_0 = [1, 1, \dots, 1]^T$, we obtain

$$\lim_{k \rightarrow \infty} \|V_l^{(k)} - V_t^{(k)}\| = \lim_{k \rightarrow \infty} \left\| \sum_{i=0}^{n-1} \lambda_i^{(k)} \mathbf{a}_i (d_{il} - d_{it}) \right\| = \lim_{k \rightarrow \infty} \left\| \sum_{i=1}^{n-1} \lambda_i^{(k)} \mathbf{a}_i (d_{il} - d_{it}) \right\| = 0 \tag{17}$$

Eq.(17) shows that the limit surfaces is C^0 continuous.

Let $V_l^{(k)}, V_t^{(k)}, V_s^{(k)}$ be the l -th, t -th and s -th components of the vertex $V^{(k)}$, and d_{il}, d_{it}, d_{is} be the l -th, t -th and s -th components of the eigenvector \mathbf{d}_i , respectively. The eigenvalues and eigenvectors satisfy $\lambda_1 = \lambda_2 = 1/45$ and $\mathbf{d}_0 = [1, 1, \dots, 1]^T$, then the normal vector of the surface defined by the three points $N_{ls \times ls}^{(k)}$ can be expressed as

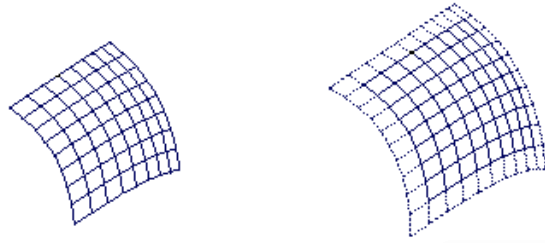
$$\begin{aligned} \lim_{k \rightarrow \infty} \frac{N_{ls \times ls}^{(k)}}{\|N_{ls \times ls}^{(k)}\|} &= \lim_{k \rightarrow \infty} \frac{(V_l^{(k)} - V_s^{(k)}) \times (V_t^{(k)} - V_s^{(k)})}{\|(V_l^{(k)} - V_s^{(k)}) \times (V_t^{(k)} - V_s^{(k)})\|} \\ &= \lim_{k \rightarrow \infty} \frac{\left(\sum_{i=0} \mathbf{a}_i \lambda_i^{(k)} d_{il} - \sum_{i=0} \mathbf{a}_i \lambda_i^{(k)} d_{is} \right) \times \left(\sum_{i=0} \mathbf{a}_i \lambda_i^{(k)} d_{it} - \sum_{i=0} \mathbf{a}_i \lambda_i^{(k)} d_{is} \right)}{\left\| \left(\sum_{i=0} \mathbf{a}_i \lambda_i^{(k)} d_{il} - \sum_{i=0} \mathbf{a}_i \lambda_i^{(k)} d_{is} \right) \times \left(\sum_{i=0} \mathbf{a}_i \lambda_i^{(k)} d_{it} - \sum_{i=0} \mathbf{a}_i \lambda_i^{(k)} d_{is} \right) \right\|} \\ &= \lim_{k \rightarrow \infty} \frac{\lambda_1^2 ((d_{1l} - d_{1s}) \mathbf{a}_1 + (d_{2l} - d_{2s}) \mathbf{a}_2) \times ((d_{1t} - d_{1s}) \mathbf{a}_1 + (d_{2t} - d_{2s}) \mathbf{a}_2)}{\lambda_1^2 ((d_{1l} - d_{1s}) \mathbf{a}_1 + (d_{2l} - d_{2s}) \mathbf{a}_2) \times ((d_{1t} - d_{1s}) \mathbf{a}_1 + (d_{2t} - d_{2s}) \mathbf{a}_2)} \\ &= \frac{\mathbf{a}_2 \times \mathbf{a}_1}{\|\mathbf{a}_2 \times \mathbf{a}_1\|} \end{aligned} \tag{18}$$

Eq.(18) shows that the limit surfaces is tangent plane continuous. Besides, the map between the control points and corresponding projections on the tangent plane is injective. According to the sufficient conditions for surface continuity^[9], we draw the conclusion that the limit surface is C^1 continuous. □

2.4 Boundaries

The previous sections present subdivision scheme for closed surfaces. However, it is often necessary to model surfaces with boundaries. For open meshes, boundary edge fails to produce a new face due to incompleteness of mask configuration, so we make use of the symmetry to create new edge vertices around the boundary edge. The new edge vertices and the old edge vertices are connected to form quadrilateral faces as shown in Fig.4. The

face-generation approach yields a complete quadrilateral mesh for arbitrary open meshes, so the new ternary subdivision masks for regular and irregular meshes can be applied again.



(a) The original mesh (b) The new mesh after adding edge vertices

Fig.4 Edge vertices on the boundary

3 Examples and Comparisons

There are some typical subdivision schemes of quadrilateral meshes: Catmull-Clark and Doo-Sabin subdivision that are based on tensor product surface, 4-8 subdivision^[11] and $\sqrt{2}$ -Subdivision^[15]. In this section, we will compare the convergence speed of our method with the existing typical methods by the eigenvalue analysis. Some examples are also given.

3.1 Convergence speed comparisons

The block matrices $S_i^{(k)}$ ($i=0, \dots, n-1$) of Catmull-Clark subdivision scheme at the k -th subdivision level can be expressed as

$$S_0^{(k)} = \begin{bmatrix} 9/16n & 3/16n & 1/16n & 3/16n \\ 3/16 & 3/16 & 1/16 & 3/16 \\ 1/4 & 1/4 & 1/4 & 1/4 \\ 3/16 & 1/16 & 1/16 & 3/16 \end{bmatrix}, S_1^{(k)} = \begin{bmatrix} 9/16n & 3/16n & 1/16n & 3/16n \\ 0 & 0 & 0 & 0 \\ 0 & 0 & 0 & 0 \\ 3/16 & 3/16 & 1/16 & 1/16 \end{bmatrix},$$

$$S_i^{(k)} = \begin{bmatrix} 9/16n & 3/16n & 1/16n & 3/16n \\ 0 & 0 & 0 & 0 \\ 0 & 0 & 0 & 0 \\ 0 & 0 & 0 & 0 \end{bmatrix}, S_{n-1}^{(k)} = \begin{bmatrix} 9/16n & 3/16n & 1/16n & 3/16n \\ 3/16 & 1/16 & 1/16 & 3/16 \\ 0 & 0 & 0 & 0 \\ 0 & 0 & 0 & 0 \end{bmatrix}.$$

The block matrices are transformed into block diagonal matrices, then we get the eigenvalues of the subdivision matrix with the relationship

$$\lambda_0=1 > \lambda_1=\lambda_2=1/4 > \lambda_{i0}=1/16 > \lambda_{i1} = \frac{1}{128\omega^i(64w^i + 4w^{2i} + 4\sqrt{131}\omega^{2i} + 46\omega^{3i} + 46\omega^i + \omega^{4i} + 1)} \geq \lambda_{i2}$$

$$= \frac{1}{128\omega^i(64w^i + 4w^{2i} - 4\sqrt{131}\omega^{2i} + 46\omega^{3i} + 46\omega^i + \omega^{4i} + 1)} > \lambda_{i3} = \lambda_{i3} = 0.$$

The eigenvalues of subdivision matrix for the Catmull-Clark subdivision scheme are bigger than those of the ternary subdivision scheme, so the ternary scheme has a faster convergence speed.

Since Doo-Sabin and Catmull-Clark schemes are based on bisection refinement, they have the same convergence speed. Note that Doo-Sabin scheme does not guarantee to generate quadrilateral meshes when the original meshes are irregular quadrilateral meshes. The 4-8 subdivision can be viewed as a $\sqrt{2}$ -subdivision when the underlying quadrilateral structure is considered during the refinement process. The $\sqrt{2}$ -subdivision scheme can also be regarded as an extension of the 4-8 subdivision directly operating upon a quadrilateral mesh. Given an

original control mesh, two bisection refinement steps of the 4-8 subdivision are equivalent to a face split of the Catmull-Clark subdivision, thus the convergence speed of the 4-8 subdivision and $\sqrt{2}$ -subdivision is slower than that of the Catmull-Clark subdivision. In consequence, the convergence speed of the ternary subdivision scheme is faster than other typical schemes.

3.2 Some examples

We have tested the new ternary subdivision scheme with a lot of different types of geometric models and some of them are given here to illustrate the performance. The comparison of Catmull-Clark scheme and the ternary scheme is shown in Fig.5.

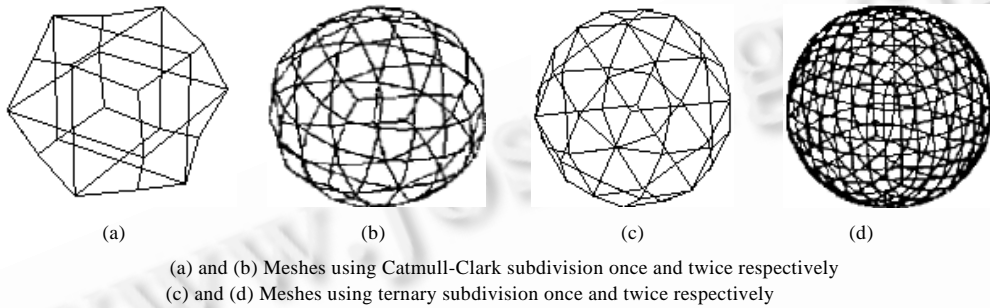


Fig.5 Comparison of Catmull-Clark and ternary scheme

In Fig.6, the original control mesh is regular quadrilateral mesh and the limit surface is C^2 using the new ternary subdivision scheme. In Fig.7, Fig.8 and Fig.9, the original meshes are irregular meshes and the limit surfaces are C^1 . Figures 6-9 show that the subdivision surfaces generated by the ternary scheme have fair and natural looks, especially in Fig.8 and Fig.9 the surfaces look smooth through four times subdivision and there is little difference between the third and the fourth subdivisions.

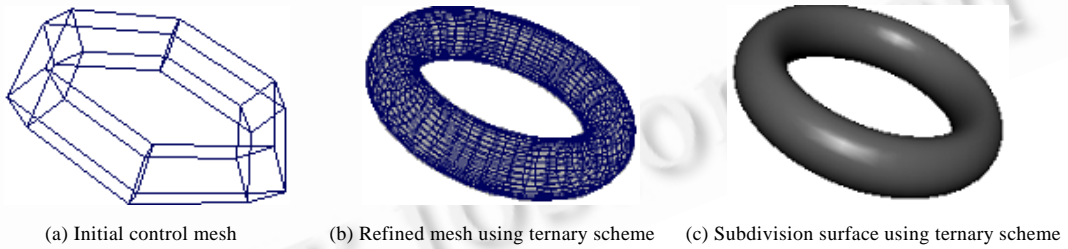


Fig.6

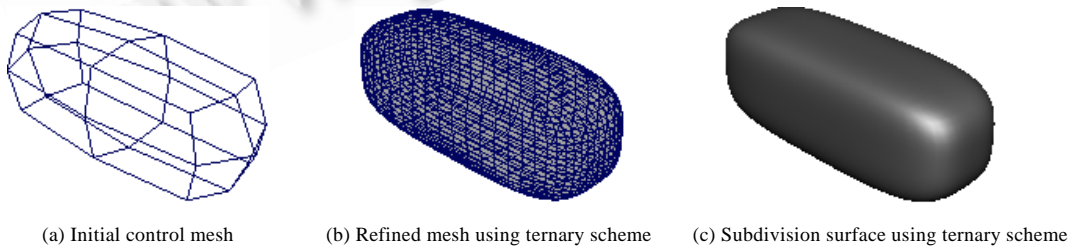


Fig.7

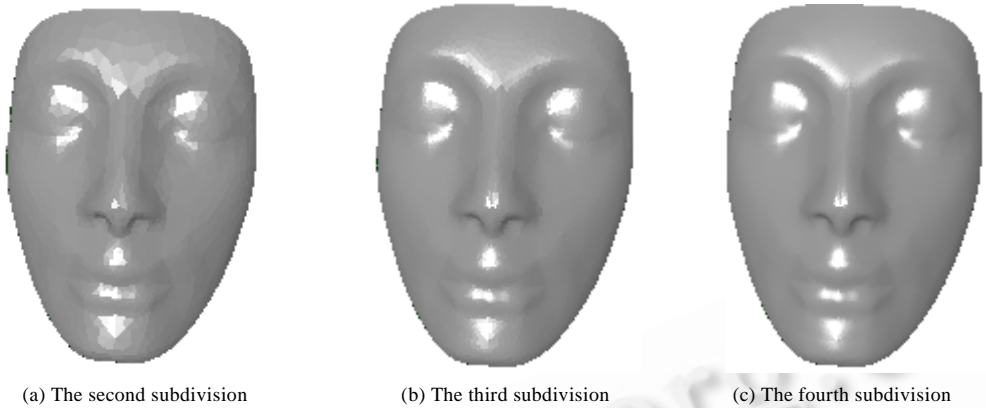


Fig.8

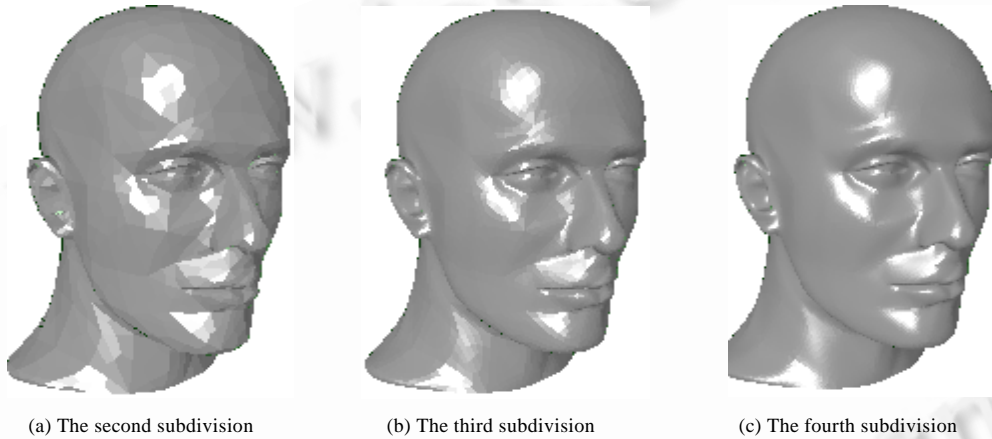


Fig.9

4 Conclusions

We present the ternary stationary subdivision scheme for regular and irregular meshes. The subdivision mask for regular mesh is deduced from bi-cubic B-spline surfaces and the subdivision mask for irregular mesh comes from face split. The limit surfaces are C^2 and C^1 continuous respectively. The face number is about nine times than that of the coarse mesh after each refinement step. The new ternary subdivision scheme has fast convergence speed and works well for both regular and irregular meshes, so it has wide adaptability. In this paper, we pay less attention to creases and object boundaries. More work is needed in those cases to improve the quality of the refined shape and sophisticated continuity analysis is also needed, which are our future research.

References:

- [1] Catmull E, Clark J. Recursively generated B-spline surfaces on arbitrary topological meshes. *Computer Aided Design*, 1978,10(6): 350-355.
- [2] Doo D, Sabin M. Behavior of recursive division surfaces near extraordinary points. *Computer Aided Design*, 1978,10(6):356-360.
- [3] Ma WY. Subdivision surfaces for CAD—An overview. *Computer Aided Design*, 2005,37(7):693-709.
- [4] Kobbelt L. $\sqrt{3}$ -subdivision. In: *Proc. of the SIGGRAPH 2000*. New York: ACM Press, 2000. 103-112.

- [5] Dyn N, Levin D, Gregory JA. A butterfly subdivision scheme for surface interpolation with tension control. *ACM Trans. on Graphics*, 1990,9(2):160–169.
- [6] Reif U. A unified approach to subdivision algorithms near extraordinary vertices. *Computer Aided Geometric Design*, 1995,12(2):153–174.
- [7] Peters J, Reif U. The simplest subdivision scheme for smoothing polyhedra. *ACM Trans. on Graphics*, 1997,16(4):420–431.
- [8] Habib A, Warren J. Edge and vertex insertion for a class of C^1 subdivision surfaces. *Computer Aided Geometric Design*, 1999,16(4):223–247.
- [9] Zorin D. Smoothness of stationary subdivision on irregular meshes. *Constructive Approximation*, 2000,16(3):359–398.
- [10] Stam J. On subdivision schemes generalizing uniform B-spline surfaces of arbitrary degree. *Computer Aided Geometric Design*, 2001,18(5):383–396.
- [11] Zorin D, Velho L. 4-8 subdivision. *Computer Aided Geometric Design*, 2001,18(5):397–427.
- [12] Zorin D, Schröder P. A unified framework for primal/dual quadrilateral subdivision scheme. *Computer Aided Geometric Design*, 2001,18(5):429–454.
- [13] Stam J, Loop C. Quad/Triangle subdivision. *Computer Graphics Forum*, 2003,22(1):1–7.
- [14] Warren J, Schaefer S. A factored approach to subdivision surfaces. *Computer Graphics & Applications*, 2004,24(3):74–81.
- [15] Li GQ, Ma WY, Bao HJ. $\sqrt{2}$ -Subdivision for quadrilateral meshes. *The Visual Computer*, 2004,20(2-3):180–198.
- [16] Hassan MF, Ivriissimitzis IP, Dodgson NA, Sabin MA. An interpolating 4-point C^2 ternary stationary subdivision scheme. *Computer Aided Geometric Design*, 2002,19(1):1–18.
- [17] Maillot J, Stam J. A unified subdivision scheme for polygonal modeling. *Computer Graphics Forum*, 2001,20(3):471–479.



LIU Li was born in 1979. She is a Ph.D. candidate. Her research areas are the area of CAD, CAGD and image processing.



YANG Xing-Qiang was born in 1964. He is an associate professor and a CCF senior member. His research areas are CAD and CAGD.



ZHANG Cai-Ming was born in 1955. He is a professor, doctoral supervisor and a CCF senior member. His research areas are CAGD, CG and medical image processing.



BO Peng-Bo was born in 1978. He is a Ph.D. candidate. His research areas are CAGD, CG and information visualization.